sustainability

MDPI

Article

Mechanisms and Resilience Governance of Built Heritage Spatial Differentiation in China: A Sustainability Perspective

Yangyang Lu [1,2,†], Longyin Teng [1,†], Jian Dai [1], Qingwen Han [2], Zhong Sun [2] and Lin Li [1,*]

[1] College of Architecture and Urban Planning, Beijing University of Technology, Beijing 100124, China; lyy891014@emails.bjut.edu.cn (Y.L.)
[2] College of Architecture, Nanyang Institute of Technology, Nanyang 473006, China
* Correspondence: lilin2015@bjut.edu.cn
† These authors contributed to the work equally and should be regarded as co-first author.

Abstract

Built heritage serves as a vital repository of human history and culture, and an examination of its spatial distribution and influencing factors holds significant value for the preservation and advancement of our historical and cultural narratives. This thesis brings together various forms of built heritage, employing methodologies such as kernel density estimation, average nearest neighbor analysis, and standard deviation ellipses to elucidate the characteristics of spatial distribution. Additionally, it investigates the influencing factors through geographical detectors and Multiscale Geographically Weighted Regression (MGWR). The findings reveal several key insights: (1) In terms of geographical patterns, built heritage is predominantly located southeast of the "Hu-Huanyong" line, with notable concentrations at the confluence of Shanxi and Henan provinces, the southeastern region of Guizhou, as well as in southern Anhui, Fujian, and Zhejiang. Moreover, distinct types of built heritage exhibit marked spatial variations. (2) The reliability and significance of the analytical results derived from prefecture and city-level units surpass those obtained from grid and provincial-level analyses. Among the influencing factors, the explanatory power associated with the number of counties emerges as the strongest, while that relating to population density was the weakest; furthermore, interactions among factors that meet significance thresholds reveal enhanced explanatory capabilities. (3) Both road density and population density demonstrate positive correlations; conversely, the positive influence of topographic relief and river density accounts for 90% of their variance. GDP exhibits a negative correlation, with the number of counties contributing to 70% of this negative impact; thus, the distribution of positive and negative influences from various factors varies significantly. Drawing upon these spatial distribution characteristics and the disparities observed in regression coefficients, this thesis delves into potential influence factors and proposes recommendations for the development and safeguarding of built heritage.

Keywords: built heritage; historical area; geographic detectors; MGWR; heritage sustainability; resilience governance

check for updates

Academic Editor: Elena Lucchi

Received: 24 March 2025
Revised: 23 June 2025
Accepted: 27 June 2025
Published: 2 July 2025

Citation: Lu, Y.; Teng, L.; Dai, J.; Han, Q.; Sun, Z.; Li, L. Mechanisms and Resilience Governance of Built Heritage Spatial Differentiation in China: A Sustainability Perspective. *Sustainability* **2025**, *17*, 6065. https://doi.org/10.3390/su17136065

Copyright: © 2025 by the authors. Licensee MDPI, Basel, Switzerland. This article is an open access article distributed under the terms and conditions of the Creative Commons Attribution (CC BY) license (https://creativecommons.org/licenses/by/4.0/).

1. Introduction

Historical and cultural heritage constitutes a critical nexus of material and spiritual value, reflecting the evolution of human civilization. The theoretical underpinnings integrate Christaller's Central Place Theory (explaining heritage agglomeration in nodal towns like Pingyao) and Steward's Cultural Ecology (deciphering Taihang Mountains' terrain–heritage symbiosis), alongside critical heritage studies and spatial analysis. Internationally,

scholars like Ashworth (1994) and Graham (2002) frame heritage as a dynamic, contested construct shaped by power dynamics [1–3]. In China, recent studies integrate Cultural Ecology theory, viewing heritage as symbiotic systems of nature and human activity [4]. Historically, Confucian ideals of continuity have influenced Chinese preservation practices, contrasting with Western emphasis on aesthetic authenticity—a dichotomy evident in debates over reconstruction versus conservation [5].

Built heritage is a synthesized construct in Chinese conservation practice, denoting human-made material legacy systems formed through labor or living activities. It encompasses four subtypes: settlements (towns/villages), structures (protected cultural relics), functional zones (historic areas), and technological facilities (industrial/agricultural heritage). While partially overlapping "Cultural Landscape" internationally, it prioritizes engineering materiality, differing from UNESCO's "Heritage Complex" that focuses on singular monuments. Spatial data cleansing rules (Section 2.1.1) resolve typological overlaps—e.g., Pingyao City Walls belong to both 'cultural relics' and 'historic districts' but are exclusively classified under the higher-protected former category—ensuring scientific synthesis of multi-types.

Globally, preservation frameworks have evolved from Europe's 19th-century monument-centric approaches to integrated paradigms emphasizing intangible and contextual values. Key milestones include the Venice Charter (1964) advocating for authenticity and UNESCO's Historic Urban Landscape (HUL) initiative (2011) [6,7], a paradigm shift from physical monuments to socio-ecological systems, directly extending Ashworth's dynamic construct into operational frameworks. China's systematic protection began with the 1982 Cultural Relics Protection Law, expanding to encompass diverse categories such as historical and cultural cities/towns/villages and industrial relics. This HUL-driven integration catalyzed China's policy evolution: while the 1982 law focused on singular relics, post-2010 expansions to towns/villages and industrial heritage explicitly internalize HUL's layered-value approach [8]. This dual trajectory—global standardization and localized adaptation—underscores the interplay between universal principles and cultural specificity.

European research highlights riverine and trade routes as heritage distribution catalysts, with clustering around medieval trade networks [5]. In Africa, studies link heritage dispersion to colonial infrastructure and post-independence urbanization [9]. U.S. scholarship emphasizes railroad expansion and deindustrialization as drivers of industrial heritage patterns. Chinese-built heritage distribution is shaped by topography and historical migration [10]. Economic factors, such as tourism investment, increasingly influence preservation outcomes, yet often exacerbate regional disparities [11]. Recent advancements include 3D digital twins for urban heritage management [12] and network analysis to map Silk Road heritage corridors [13]. Innovations like AI-driven predictive modeling and participatory GIS are reshaping the field [14]. However, challenges remain in standardizing cross-cultural data and addressing climate change impacts on heritage resilience [15].

Existing nationwide studies predominantly analyze spatial patterns of mono-typological elements (e.g., traditional villages or industrial relics) or face comparability constraints from sub-national scales (e.g., provincial density metrics distorted by administrative area disparities). Representative studies include a study by Wang Rong, who analyzed the spatial distribution and driving factors of historical and cultural towns/villages through basic spatial statistics methods [16]. Scholars have researched the spatial distribution characteristics and influencing factors of traditional villages at the national level [17], provincial level [18–20], and special zoning levels [10,21–24]. Xi Xuesong analyzed the spatial distribution characteristics of cultural heritage sites from the perspectives of history, types, and natural and cultural geography regions [25]. Ma Mengyao et al. analyzed the spatial distribution of industrial heritage at the national level [4]. Thus, by integrating four heritage

categories (Section 2.1.1) with standardized density metrics across 31 provinces, this study pioneers comparable cross-scale analysis for multi-typological heritage—resolving the dual limitations of 'mono-typological narrowness' and 'regional data incomparability' in the extant literature.

In terms of research methods for spatial distribution, early studies used spatial overlay or buffering techniques for classification, zoning, and statistical analysis [16,26]. They also employed spatial statistical methods such as kernel density analysis, nearest neighbor index [27], geographic concentration index [28], standard deviation ellipse, and spatial autocorrelation [4]. In terms of influencing factors, there are mainly two categories: natural and human factors, including terrain, climate, economy, society, culture, and transportation [29,30]. In the analysis of influencing factors, qualitative descriptions have been commonly used. However, with the development of geographic spatial analysis methods, some scholars have quantified indicators such as terrain, population/population density, GDP, and road network density, and used geographic detectors to explore the impact of different factors on single types of built heritage [31,32]. Geographic weighted regression has been employed to investigate the local effects of factors in geographic space. In summary, the academic research on built heritage lacks scientific comparative arguments regarding the division of research units at different scales. The research objects are too singular, which does not align well with the trend of diversification and systematization in China's historical and cultural heritage preservation and inheritance system. Therefore, it is necessary to conduct a comprehensive study on multiple types of built heritage.

In summary, academic research on built heritage faces three critical gaps: (1) scale fragmentation, neglecting transregional interactions; (2) temporal blindness, with static methods failing to capture dynamic degradation; and (3) theory–practice divide, particularly in non-Western contexts where critical heritage theory rarely intersects with quantitative spatial analysis [33].

This study addresses these gaps by synthesizing multi-type heritage (historical districts, villages, and industrial sites) into a unified geodatabase, enabling cross-category analysis via geographical detectors and MGWR. By integrating Chinese cases with global paradigms, it reveals local anomalies challenging universal models. Methodologically, it pioneers participatory GIS and temporal–spatial models for dynamic preservation planning. Methodologically, these contributions advance heritage research toward holistic, adaptive systems embedded in evolving socio-environmental landscapes, offering policymakers tools to balance preservation with sustainable development.

2. Materials and Methods

2.1. Study Subjects

2.1.1. Data Resources

This study employs three core datasets for spatial analysis: (1) administrative boundaries: vector boundaries of national/provincial/prefectural units (1:1 M scale, 2023) from the Resource and Environment Science Data Center (RESDC); (2) dependent variable: geospatial database of China's built heritage; (3) independent variables: natural and socioeconomic driving factors.

The built heritage database integrates four authoritative inventories: (1) historic areas (1239 sites): compiled from official portals of 31 provincial administrations (no centralized national repository); (2) protected cultural relics (27,309 sites): National Key Cultural Relics Protection Units Catalogue (2023) by State Administration of Cultural Heritage (SACH); (3) settlement heritage (9456 sites): historic towns/villages list (2022) (312 towns + 487 villages) + traditional villages directory (2023 supplement) (8155 sites) by the Ministry of Housing and Urban–Rural Development (MOHURD), PRC; (4) functional heritage (276 sites): List of Industrial Heritage (2024) (199 sites) by the Ministry of Industry and Information Technology (MIIT), PRC+ Agri/Irrigation Heritage Bulletin (2023) (77 sites) by Ministry of Agriculture and Rural Affairs and Ministry (MARA), PRC of Water Resources (MWR), PRC. Data deduplication protocol: (a) single-location heritage retains only the highest protection-level category; (b) cross-scale heritage (e.g., provincial relics within national villages) adopts macro-typology to avoid micro-duplication.

Independent variable sources: (1) socio-economic: RESDC *1 km-grid Spatial GDP/Population Dataset (2020)*; (2) terrain: 30 m ASTER GDEM v3 (2022) from Geospatial Data Cloud; (3) infrastructure: RESDC National Highway Vector Dataset (2023); (4) hydrology: River Basin Network Dataset (2021) from the Ministry of Water Resources; (5) statistical baseline: NBS China Statistical Yearbook 2023.

2.1.2. Type Classification

There are many types of built heritage in China. Based on the form of protection, it can be classified into protection focusing on individual units, areas, and whole entities. In terms of morphology, it can be categorized into point-like, linear, and multifaceted forms. According to functional types, it can be divided into residential, commercial, industrial, agricultural, public utility, and comprehensive types. This paper identifies China's built heritage into four types, taking into account the development of historical and cultural heritage protection. The first type is a historical settlement that has adopted an overall conservation model, including Chinese traditional villages, historical and cultural villages, and towns. The second type is cultural relic protection units, which are protected as a single unit, including national and provincial cultural relics protection units. The third type is the historical area, which takes the area as the object of protection, including the historical conservation area, historical area, and historical landscape area. The fourth type is published and declared historical heritage with special functions, including industrial heritage, agricultural heritage, and irrigation heritage.

2.2. Research Methodology

At the national geographical scale, all built heritage can be conceptualized as discrete point elements, whose geographic coordinates and numerical data serve as fundamental parameters for analysis. Upon importing this data into ArcGIS 10.8, we examined the spatial characteristics and influencing factors through a systematic three-step process: (1) kernel density estimation and average nearest neighbor analysis were employed to ascertain the spatial distribution and patterns of built heritage; (2) kernel density estimates, standard deviation ellipses, and mean centers were utilized to investigate the variations in the center, extent, and directional distribution of different types of built heritage; and (3) a geographical detector alongside Multiscale Geographically Weighted Regression (MGWR) was applied to identify and evaluate the driving factors underlying the evolution of built heritage.

2.2.1. Kernel Density Analysis

A kernel density analysis measures local concentration while accommodating heterogeneity—via adaptive bandwidths (h) that expand in sparse areas and contract in dense zones, per Silverman's rule (1986), providing a clear reflection of the spatial distribution characteristics of the research elements. In this study, it is used to analyze the dispersion and clustering of built heritage. The expression formula is as follows:

$$f_n(x) = \frac{1}{nh}\sum_{i=1}^{n} k\left(\frac{x - x_i}{h}\right) \tag{1}$$

where $f_n(x)$ is the kernel density estimate, the $k\left(\frac{x-x_i}{h}\right)$ is the kernel function, x_i is the coordinate of the point to be calculated, h is the search bandwidth distance, and n is the number of built heritages. A larger $f_n(x)$ indicates a denser distribution of point elements, while a smaller value indicates a more dispersed distribution.

2.2.2. Average Nearest Neighbor

The index evaluates clustering with Monte Carlo simulations controlling terrain fragmentation—e.g., mountain heritage shows pseudo-clustering due to isolation vs. true clustering in plains. The method determines the spatial distribution pattern of built heritage by measuring the average of the sum of the distances from the center of mass of each built heritage to the built heritage of its nearest neighbors and then comparing it to the average distance of an assumed random distribution:

$$D_o = \frac{1}{n}\sum_{i-1}^{n} d_i, D_e = \frac{1}{2\sqrt{\frac{n}{A}}} \tag{2}$$

$$R = \frac{D_o}{D_e} \tag{3}$$

where d_i is the distance from each element to its nearest built heritage and n is the total number of built heritages. D_o is the average nearest neighbor distance between each built heritage and its nearest built heritage, D_e is the expected nearest neighbor distance between each built heritage and its nearest built heritage, and A is the total study area.

2.2.3. Standard Deviation Ellipse

The standard deviation ellipse is the axis of the ellipse that contains all the elements by measuring the standardized distances of different types of built heritage in the X and Y directions separately from the global spatial perspective. Specifically, the main trend direction of the distribution of different types of built heritage is determined by the ellipse orientation, with the long axis indicating the direction of maximum diffusion and its diffusivity and the short axis indicating the direction of minimum diffusion, as computed in Equations (5)–(7). By superimposing the four forms of the ellipse, the distribution law of built heritage can be studied in terms of both scope and direction:

$$SDE_x = \sqrt{\frac{\sum_{i=1}^{n}\left(x_i - \overline{X}\right)^2}{n}}, \; SDE_y = \sqrt{\frac{\sum_{i=1}^{n}\left(y_i - \overline{Y}\right)^2}{n}} \tag{4}$$

$$\sigma_x = \sqrt{2}\sqrt{\frac{\sum_{i=1}^{n}\left(\widetilde{x}_i\cos\theta - \widetilde{y}_i\sin\theta\right)^2}{n}}, \; \sigma_y = \sqrt{2}\sqrt{\frac{\sum_{i=1}^{n}\left(\widetilde{x}_i\sin\theta - \widetilde{y}_i\cos\theta\right)^2}{n}} \tag{5}$$

$$\tan\theta = \frac{\left(\sum_{i=1}^{n}\widetilde{x}_i^2 - \widetilde{y}_i^2\right) + \sqrt{\left(\sum_{i=1}^{n}\widetilde{x}_i^2 - \sum_{i=1}^{n}\widetilde{y}_i^2\right)^2 + 4\left(\sum_{i=1}^{n}\widetilde{x}_i\widetilde{y}_i\right)^2}}{2\sum_{i=1}^{n}\widetilde{x}_i\widetilde{y}_i} \quad (6)$$

where x_i,y_i are the center coordinates of each legacy, $\widetilde{x}_i$, $\widetilde{y}_i$ is the difference between the mean center and the X and Y coordinates of the i-th built heritages, θ is the elliptical azimuth (the angle formed by rotating from due north along the clockwise direction to the main axis), $\overline{X}$, $\overline{Y}$ are the arithmetic mean centers, and n is the total number of different types of built heritages.

2.2.4. Geographical Detectors

A geographical detector is an analysis method that explores the spatial heterogeneity distribution and influencing factors of geographic spatial elements by examining the spatial similarity between independent and dependent variables [34]. Geographical detectors include four detectors. In this study, the differentiation and factor detector and interaction detector are used to analyze the effects of various influencing factors on the spatial distribution of built heritage. The calculation formula is as follows:

$$q = 1 - \frac{\mathrm{SSW}}{\mathrm{SST}} = 1 - \frac{\sum_{h=1}^{L} N_h\sigma_h^2}{N\sigma^2} \quad (7)$$

where $q = 1, \ldots, L$ is the partition of the dependent variable (built heritage) or the independent variables (influencing factors); N_h and N are the number of units in layer h and the total area; σ_h^2 and σ^2 a are the variances of the dependent variable in layer h and the total area; SSW and SST are the within-layer variances and the total variance of the entire area; and q ranges from 0 to 1, with larger values indicating stronger explanatory power of the independent variable on the dependent variable and smaller values indicating weaker explanatory power. The interaction detector is used to evaluate whether the joint effect of two factors enhances or weakens the explanatory power of the dependent variable.

2.2.5. Multiscale Geographic Weighted Regression

MGWR advances traditional GWR by addressing scale heterogeneity—a key limitation in heritage studies where factors like terrain (bandwidth = 50 km) and economy (bandwidth = 348 km) operate at divergent scales [35]. This aligns with multiscale spatial process theory, overcoming GWR's single-bandwidth bias [36–39]. It is represented as follows:

$$Y_i = \beta_{i0} + \sum_k \beta_{ik} X_{ki} + \varepsilon_i, \quad i = 1, 2, \ldots, n. \quad (8)$$

$$Y_i = \beta_{i0,b} + \sum_k \beta_{ik,b} X_{ki} + \varepsilon_i, \quad i = 1, 2, \ldots, n. \quad (9)$$

Equation (8) is a classical geographically weighted regression model, where β_{ik} is the regression coefficient corresponding to the sample point i concerning the kth independent variable, ε_i is the random error term, k is the following table of the independent variable parameters, and n is the sample size to be calculated. Equation (9) is a multiscale geo-weighted regression model, where $\beta_{ik,b}$ denotes the regression coefficient of the kth variable under the b-bandwidth condition, and the remaining quantitative values have the same meaning as in Equation (8).

3. Results

3.1. Structural Characteristics

The number distribution of built heritage in different provinces was counted, as illustrated in Figure 1 (middle). In terms of provinces, regions with profound historical and cultural accumulation and diverse geographical settings, such as Shanxi, Zhejiang, Hunan, and Yunnan, have the largest number of built heritages, which is more than 1000. This is followed by 11 provinces, namely Anhui, Fujian, Guangdong, Guangxi, Henan, Guizhou, Hebei, Hubei, Jiangxi, Shaanxi, and Sichuan, with a total of 500–1000. Conversely, historically less densely populated frontier regions and areas undergoing rapid modern urbanization, like Tianjin and Ningxia, were the only two provinces with a total of less than 100 (Figure 1 (middle)). In terms of built heritage types, the province with the highest distribution of cultural relics protection units is Shanxi, the province with the highest distribution of heritage published is Sichuan, the province with the highest distribution of historic settlements is Yunnan, and the province with the highest number of historic areas is Guangdong. At the municipal level, Chongqing, Qian-Southeast in Guizhou province, Jinzhong in Shanxi province, Huangshan of Anhui province, and Lishui of Zhejiang province have the largest distribution of built heritage (Figure 1 (down)).

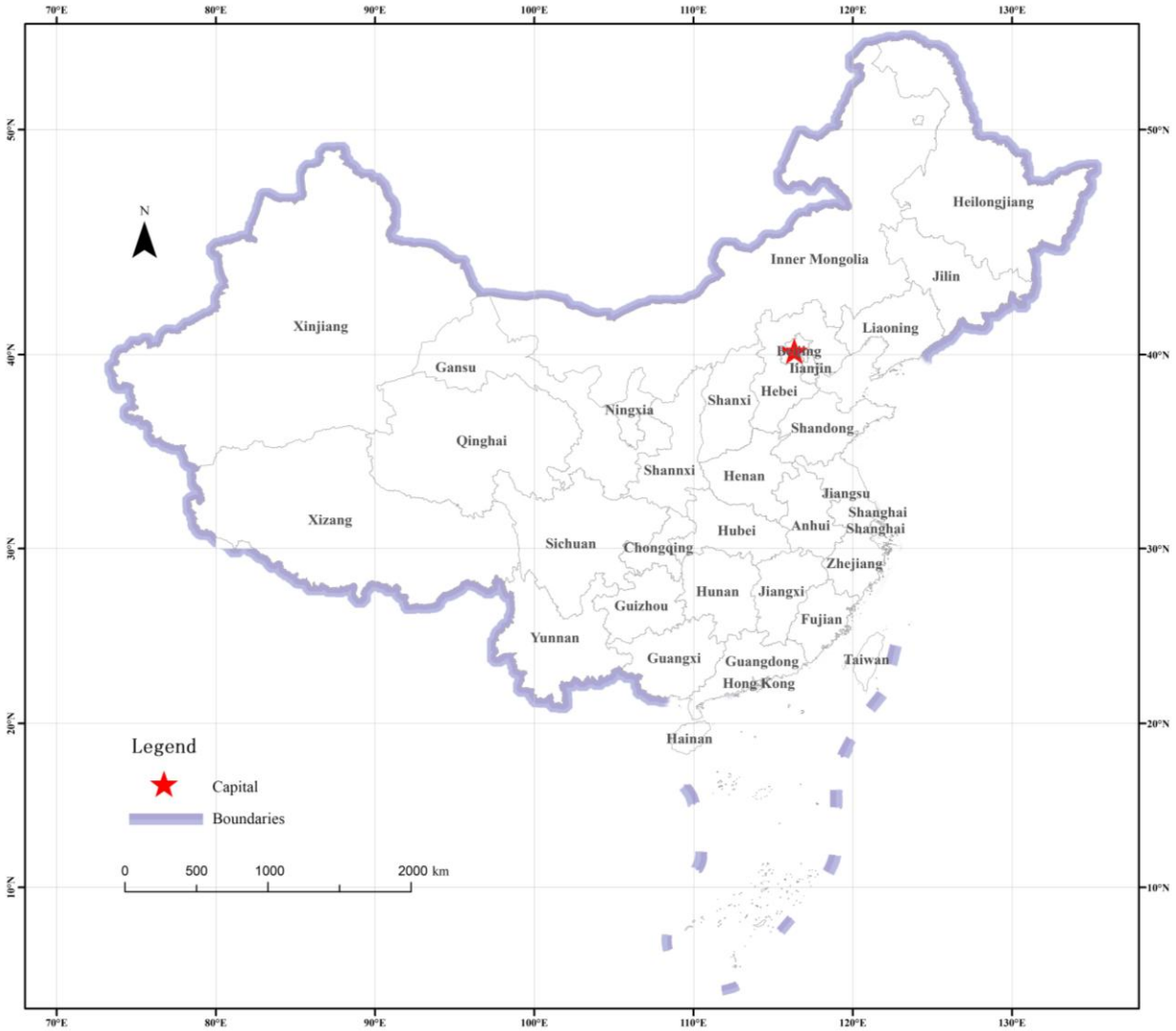


Figure 1. *Cont.*

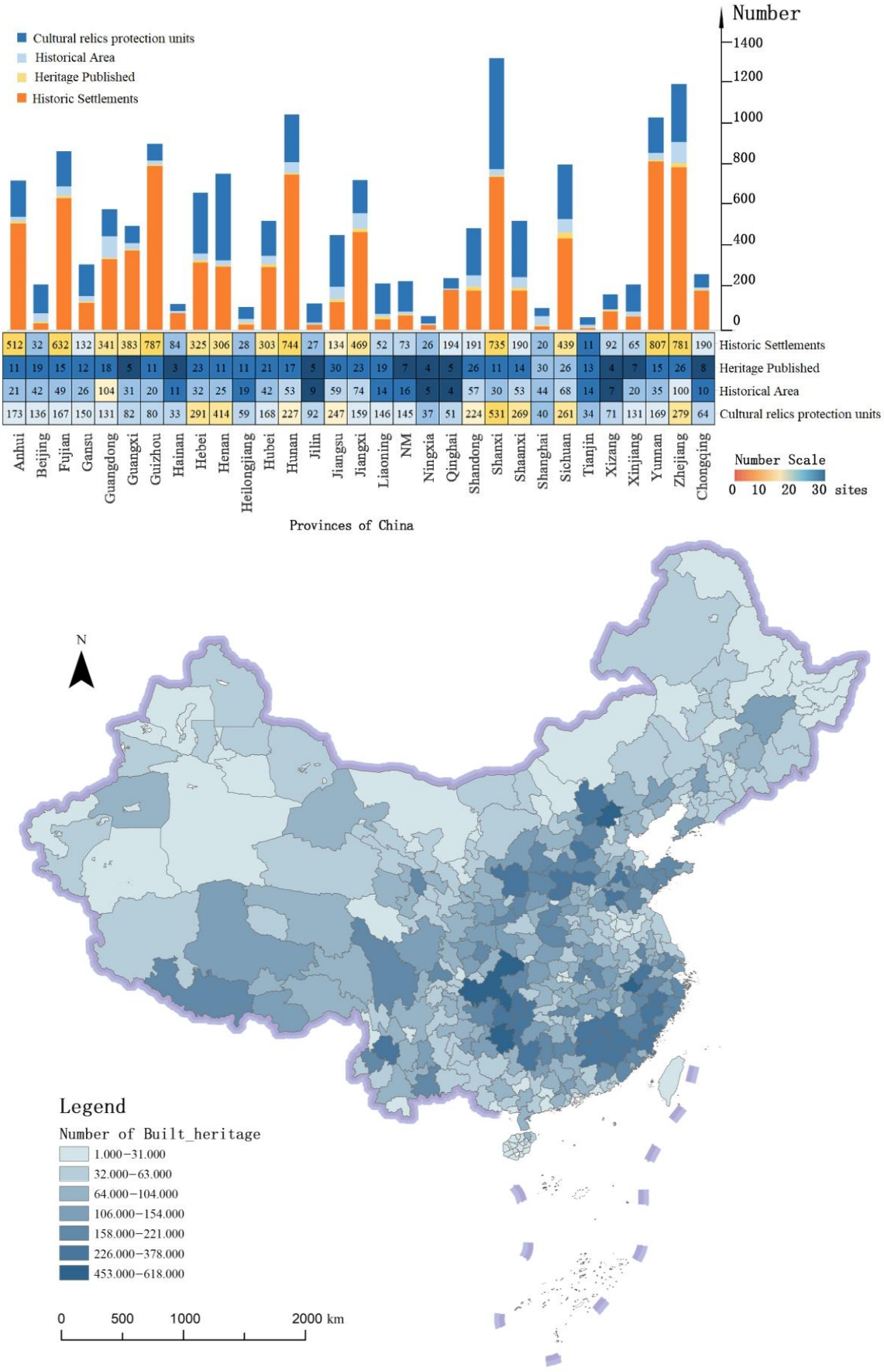


Figure 1. Location map and Structural (**up**); numbers in different cities (**middle**); number of each type in different provinces (**down**).

3.2. Spatial Distribution Characteristics

3.2.1. Distribution Characteristics from the Holistic Perspective

Spatial distribution characteristics of built heritage, including density and pattern, were calculated by a kernel density analysis, average nearest neighbor, and standard deviation ellipse in ArcGIS 10.8. The results of the kernel density analysis and the average nearest neighbor index show that built heritage is widely but unevenly distributed across the country, with a z-score of −234.8084 (Table 1), and forms four high-density core areas and several medium-density core areas in the country (Figure 2). In addition, the analysis of the standard deviation ellipse shows that the built heritage is distributed in the Northeast–Southwest direction ($\theta = 76.3362$) (Table 2), and the mean center is located in Xiangyang in Hubei (Figure 3).

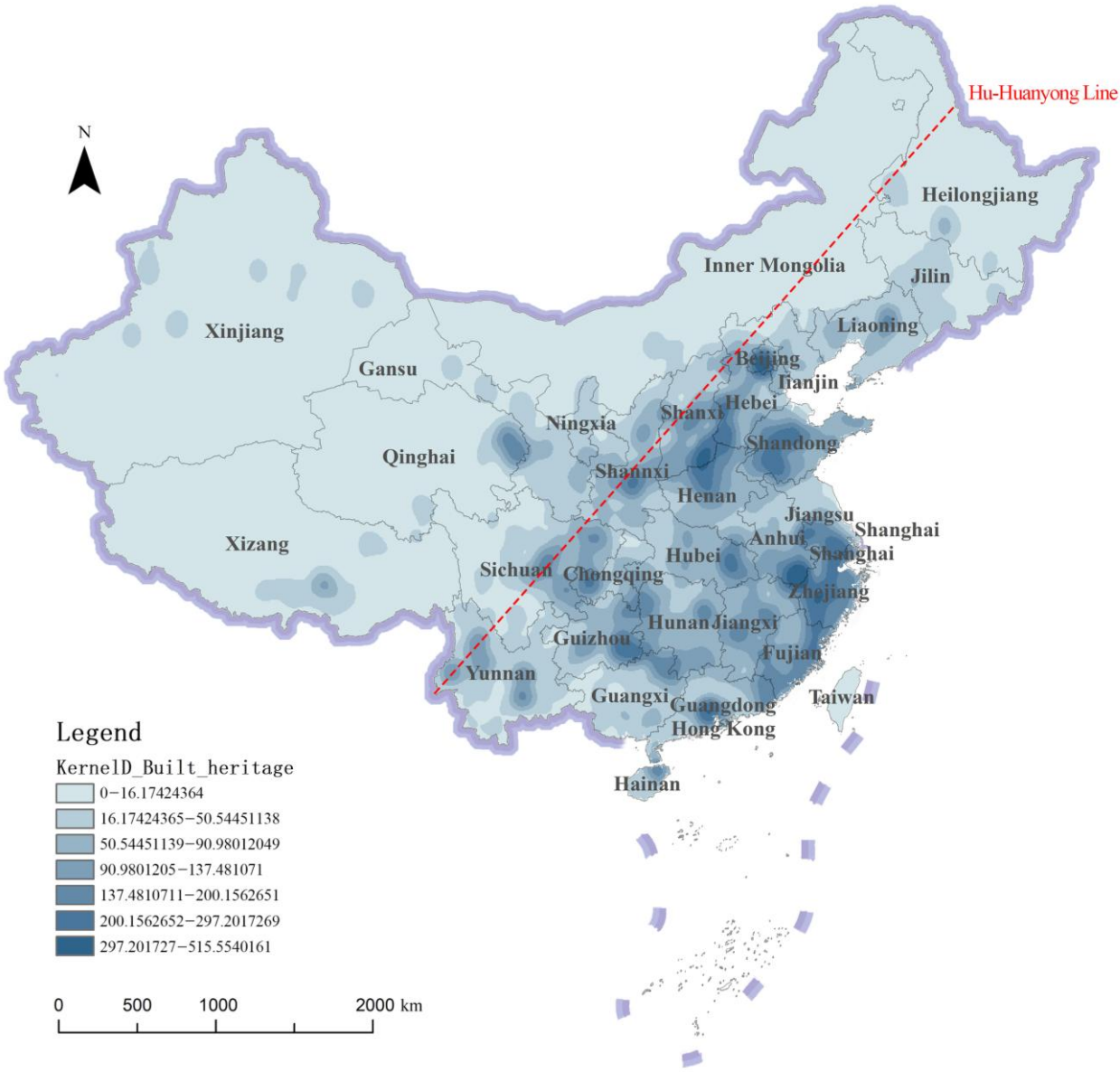


Figure 2. Kernel density of built heritage in China.

Table 1. Parameters of the standard deviation ellipse of the built heritage distribution for each type.

Type	Long Axis of Ellipse (m)	Short Axis of the Ellipse (m)	Area (m^2)	Length(m)	Azimuth Angle	Oblateness
Historic area	1,037,036.8237	825,768.4497	3,906,221,453,537.273926	7,021,754.7104	78.5904	0.2037
Historical settlements	979,343.8282	696,234.3588	3,055,951,311,432.331543	6,251,281.0282	79.8695	0.2891
Cultural relics protection units	1,170,703.1217	794,993.1693	4,298,081,379,997.493652	7,433,228.5215	77.2492	0.3209
Heritage published	1,098,915.3931	801,878.9357	4,135,865,702,469.535645	7,279,208.1098	68.0560	0.3351
Built heritage	1,119,228.8741	785,407.7433	4,024,359,535,685.680176	7,179,338.5793	76.3362	0.2986

Table 2. Global average nearest neighbor results for typological and holistic conditions.

Type	R	z-Score	*p* Score	Average Nearest Neighbor Distance (m)	Expected Nearest Neighbor Distance (m)	Distribution Pattern
Historic area	0.2280	−48.9473	0.0000	12,731.8433	55,790.2846	Significant clustered
Historical settlement	0.3297	−122.4024	0.0000	7031.6029	21,327.9519	Significant clustered
Cultural relics protection unit	0.3311	−190.2249	0.0000	4710.0392	14,222.0980	Significant clustered
Heritage published	0.4068	−24.3128	0.0000	84,993.4585	34,575.7276	Significant clustered
Built heritage	0.3232	−234.8084	0.0000	3768.8236	11,662.6557	Significant clustered



Figure 3. Distribution of standard deviation ellipses with mean center for the different types of built heritage.

The first high-density region is a belt-shaped region extending from the western part of Huangshan in Anhui (KD_M = 490.2810) to the southwestern part of Jinhua in Zhejiang (KD_M = 317.7497). The second high-density region is a point-shaped region centered around Beijing (KD_M = 381.5436). The third high-density region is a belt-shaped region extending from the western part of Zhengzhou in Henan to the central-western part of Jincheng in Shanxi, and further southeast to the western part of Changzhi in Shanxi, and the western part of Handan in Hebei (KD_M = 352.8276). The fourth high-density region is a point-shaped region centered around the south of the border between Guangzhou and Foshan in Guangdong (KD_M = 302.4740). The several medium-density cores are point-shaped areas

centered on Qiandongnan in Guizhou, Suzhou in Jiangsu, the border between Xianyang and Xian in Shaanxi, the border between Guilin in Guangxi and Yongzhou in Hunan, the western part of Xiangxi in Hunan, and Fuzhou in Fujian.

From a geographical pattern perspective, the median and high-value areas are concentrated in the Taihang Mountains, Daba Mountains–Xuefeng Mountains, and the Wuyi Mountain range, which mark the boundaries between the second and third tiers of China's topographic hierarchy. From an analysis of the population and economic patterns, the majority of China's built heritage is located east and south of the "Hu-Huanyong Line" (Figure 2).

3.2.2. Distribution Characteristics from the Typological Perspective

Spatial distribution characteristics, including density and pattern, were calculated by the nearest neighbor method (Table 2), kernel density estimation (Figure 4), and standard deviation ellipse (Figure 3 and Table 1). The result of the average nearest neighbor showed that all built heritage, as well as all subtypes, exhibit different degrees of clustering (Table 1). The highest z-score (z = −190.2249) and the strongest clustering were found for cultural relics protection units, followed by historic settlement (z = −122.4024) and historic area (z = −48.9473), and the weakest z-score was found for heritage published (z = −24.3128). The result of kernel density estimates shows that the spatial distribution of different types of built heritage varies considerably.

The historical settlement formed three high-density core areas (Figure 4a). The first is a zone centered in western Jinzhong, Shanxi province (mean kernel density KD_M = 154.1531), extending southeast to western Changzhi, Shanxi province, and western Handan, Hebei province. The second is a belt area centered on western Huangshan in Anhui province (KD_M = 227.8567), extending southwestward to west-central Jinhua in Zhejiang province, and then southward to Ningde in Fujian province. The third is a point-like region centered on Qiandongnan, Guizhou province (KD_M = 197.5329). The analysis of the standard deviation ellipse shows that the historical settlement is distributed in the Northeast–Southwest direction (θ = 79.8695) (Table 2), and the mean center is located on the border between Jingzhou in Hubei and Changde in Hunan (Figure 3).

The cultural relics protection units formed three high-density cores (Figure 4b). The first is a point-shaped area centered around Beijing (KD_M = 240.4984). The second is a large belt-shaped area extending westward from Jiaozuo, Zhengzhou in Henan, Jincheng and southern Changzhi in Shanxi, through Yuncheng in Shanxi to Xi'an and Xianyang in Shaanxi (KD_M = 188.4978). The third is a loop-shaped area in the Yangtze River Delta (KD_M = 187.1513). The analysis of the standard deviation ellipse shows that the cultural relics protection units are distributed in the Northeast–Southwest direction (θ = 77.2492) (Table 2), and the mean center is located in the south of Nanyang in Henan (Figure 3).

The historic areas formed three high-density core areas (Figure 4c). The first is a point-shaped area centered around Shanghai, Suzhou in Jiangsu province, Wuxi Jiaxing, Shaoxing, and northwestern Ningbo in Zhejiang province (KD_M = 19.8522). The second is a point-shaped area centered around Guangzhou, Foshan, and Zhongshan in Guangdong province (KD_M = 22.2297). The third is a point-shaped area centered around Beijing (KD_M = 12.7756). The analysis of the standard deviation ellipse shows that the historic areas are distributed in the Northeast–Southwest direction (θ = 78.5904) (Table 2), and the mean center is located on the border between Suizhou and Xiaogan in Hubei (Figure 3).

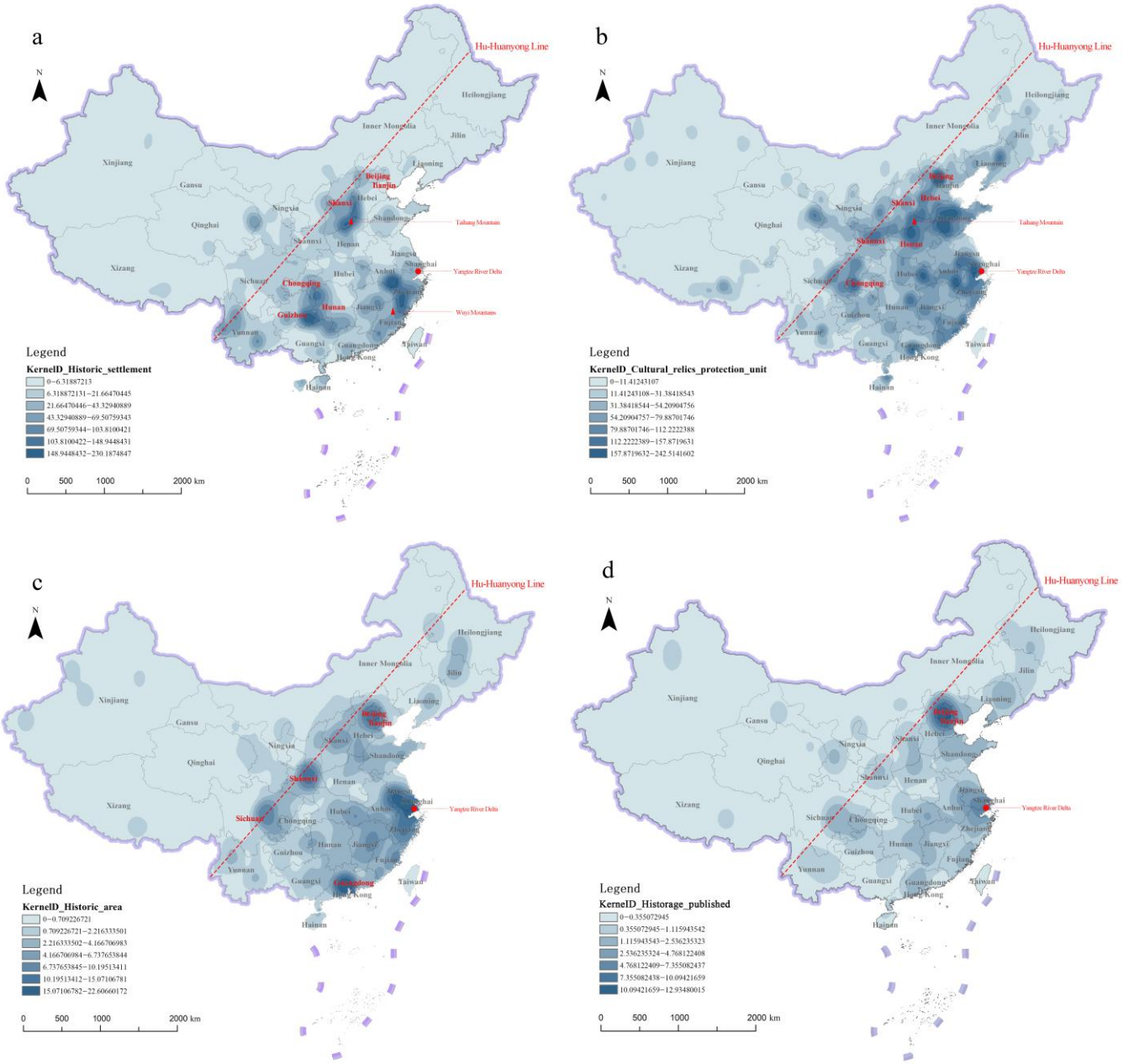


Figure 4. Results of kernel density analysis of historic settlement (**a**), cultural relics protection unit (**b**), historic area (**c**), and heritage published (**d**).

The heritage published formed two high-density cores and four medium-density core areas nationwide (Figure 4d). The first is a point-shaped area centered around Suzhou, Wuxi, Changzhou in Jiangsu, Huzhou, Jiaxing, and northeastern Hangzhou in Zhejiang (KD_M = 7.3098). The second is a point-shaped area centered around Beijing, Langfang in Hebei, and the western part of Tianjin (KD_M = 12.7177). The analysis of the standard deviation ellipse shows that the heritages published are distributed in the Northeast–Southwest direction (θ = 68.0560) (Table 2), and the mean center is located in the south of Nanyang in Henan (Figure 3).

A comprehensive comparison of the distribution characteristics of the four types of built heritage reveals that the Beijing-Tianjin is the high-density core of cultural relics protection units (Figure 4b), historic area (Figure 4c), and heritage published (Figure 4d), and the Yangtze River Delta is the high-density core of the three types of historic settlements, cultural relics protection units, and historic areas at the same time (Figure 4a–c).

In addition, Shanxi is the high-density core of the two types of historic settlements and heritage published, and west of Chongqing, Hunan, and Guizhou are the high-density cores of historic settlements and heritage published at the same time (Figure 4a,d).

3.3. Factors Influencing the Spatial Distribution

3.3.1. Selection of Impact Factors and Analysis Unit

Built heritage is the product of the comprehensive influence of the development process of modern urbanization, which is the historical remains of human settlement. Variable selection adheres to a theory–policy–empiricism tripartite framework: terrain relief grounded in Human–Environment Theory [40], GDP reflecting Spatial Production Theory [41], county count variable aligning with China's three-tier heritage designation, while other variables were pre-screened by Geodetector ($q > 0.05$) and consistent with national studies (Table 3).

Table 3. Description of explanatory variables and indicators.

Influencing Factors	Indicators	Calculation Method		Unit	Pre-Action Direction
		Grid Scale	Provincial/Municipal Scale		
Topographical	Topographic fluctuation	ArcGIS raster extraction	NSO data	m	+
	River density	Gridded river miles/gridded area	Miles of waterway/area of administrative districts	km/km^2	+
Traffic	Road density	Gridded road miles/gridded area	Road mileage/area of administrative districts	km/km^2	-
Demographic	Population	ArcGIS raster extraction	NSO data	Individual	-
	Population density	Gridded population/gridded area	Total population/area of the district	pcs/km^2	-
Urban	Urbanization rate	ArcGIS raster extraction	NSO data	%	-
	Number of districts	NSO data	NSO data	Individual	+
Economic	GDP	ArcGIS raster extraction	NSO data	Million	+
	GDP per capita	GDP/population	GDP/population	Yuan	+

In terms of formation conditions, natural geographic factors play a decisive role in the emergence of human settlement, with topography and water sources being one of the important factors influencing the human living environment [42,43] (Table 3). The explanatory variables were selected with reference to the research results of scholars on traditional villages at different levels, historically and culturally famous villages in China [16], industrial heritage [44], and other spatial distribution influencing factors. Research on topographical factors has shown that elevation has a stair-like effect on human settlements, and topographical fluctuation is a continuous influencing factor at different elevation segments. In this article, the degree of topographic relief was chosen as a factor to explain the topography of the spatial distribution of the study object. In addition, the literature analysis found that most of the previous studies analyzed the influence of spatial elements on the spatial distribution through the number of spatial elements in different levels of buffer zones of the river, which could not cover all the spatial elements, and it is not easy to make quantitative comparisons on the same scale with other research units by using buffer zones as a research unit, which is not conducive to the exploration of the interactions among the influencing factors; therefore, the present study tries to use the density of the river as one of the topographic element factors for the spatial distribution of research objects. Therefore,

this study tries to use river density as another topographic factor to explain the spatial distribution of the study object.

In addition to natural geography, transportation has also had a great impact on the emergence and development of settlements. In the early stage of settlement formation, transportation was a limiting factor for the development of settlements. With the acceleration of urbanization, rapid transportation, as a representative of modern urban development, has impacted the historic settlement pattern, thus affecting the completion and preservation of built heritage. Therefore, this article takes the road network density among the transportation factors as one of the explanatory variables to explain the spatial distribution of the research object. In addition, the evolution of settlements was always affected by population and economy. This article selects population and economic factors as variables explaining the spatial distribution of the research object. Among them, two indicators, total population and population density, are selected for demographic factors, and two factors, GDP and GDP per capita, are selected for economic factors.

After the formation of a settlement, urbanization has a multifaceted impact on its spatial pattern, historical features, and traditional culture. The urbanization rate, as a comprehensive indicator of urbanization development, has a representative impact on the distribution of built heritage. In addition, the process of declaring traditional Chinese villages and towns, such as famous historical and cultural villages and towns, starts from the lower administrative units (mainly at the county and district levels) and then goes up to the higher levels for approval. Therefore, the number of administrative units at the county and district level affects the number of built heritages in the region to a certain extent, so the article includes it as one of the urban factors to be studied (Table 3).

Variable measurement adheres to triple standardization: (1) spatial-scale normalization—e.g., road density as 'total road length/administrative area' (km/km^2) to offset provincial size effects; (2) temporal anchoring—all socio-economic data referenced to 2020 (7th National Census baseline); (3) heritage weighting—each site counts as one point regardless of type (Section 2.1.2 definitions).

The geographical detector requires dividing the study objects into different analysis units, and different division methods yield different detection results. Higher analysis unit density leads to higher precision but also increases computational load. Currently, in the use of geographical detectors at the national level, provinces are mostly chosen as analysis units [45,46], while a small number of studies use cities or grid cells for geographical detection. The geographical detector was used with historical and cultural spatial element quantity as the dependent variable, and the nine explanatory variables were geographically detected at different scales. The results show that the detection results with provinces as analysis units have only two variables that satisfy the significance level test ($p < 0.05$). Detection results using the grid image element as the unit of analysis showed that seven variables satisfied the significance level test, but none of the effects of multiple explanatory variables were significant. The results of the tests using the city as the unit of analysis indicate that seven variables satisfy the test of significance, and the explanatory power and variability of the variables are significant (Table 4). In summary, the detection accuracy of the experiment is highest when cities are used as analysis units, which balances significance and explanatory power.

Table 4. Comparison of detector results at different scales.

Independent Variable	Provincial Scale			Grid-Scale (50 × 50 km)			Municipal Scale			
	q-Value	*p*-Value and Significance Level		q-Value	*p*-Value and Significance Level		q-Value and Ranking of Explanatory Power		*p*-Value and Significance Level	
Topographic fluctuation	0.1053	0.6285	——	0.0094	0.0000	0.01	0.1363	4	0.0000	0.01
River density	0.3696	0.0130	0.05	0.0451	0.0000	0.01	0.1062	5	0.0000	0.01
Road density	0.2975	0.1053	——	0.1299	0.0000	0.01	0.0597	7	0.0105	0.05
Population	0.4806	0.0183	0.05	0.0030	0.0208	0.05	0.1448	2	0.0000	0.01
Population density	0.0453	0.5887	——	0.0030	0.0208	0.05	0.0938	6	0.0000	0.01
Urbanization rate	0.1697	0.1934	——	0.0047	0.0000	0.01	0.0230		0.4587	——
Number of counties	0.2933	0.2289	——	0.0020	0.0654	——	0.2354	1	0.0000	0.01
GDP	0.3183	0.0734	——	0.0040	0.0216	0.05	0.1398	3	0.0000	0.01
GDP per capita	0.1095	0.5914	——	0.0003	0.8343	——	0.0149		0.7755	——

Note: "——" indicates that the q-value did not pass the significance test; only the explanatory power of the independent variables that passed the significance test is ranked.

3.3.2. Single-Factor Detection Results

For individual factors, the most significant and strongest coupling was the number of counties (q = 0.2345). The second level is population (q = 0.1448), GDP (q = 0.1398), and topographical fluctuation (q = 0.1363), which do not have much difference in their explanatory power, and all of them are located in the range of 1.3–1.5. The third level was river density (q = 0.1062) and population density (q = 0.0938), whose q values are nearly 1.0. The lowest significant coupling was road density, with q values of 0.0597 and *p* values of 0.01 to 0.05. These results indicate that the spatial distribution of built heritage by the city units is more influenced by administration, transportation accessibility, and socio-economic factors, and less associated with population density and road network density (Table 4).

3.3.3. Interaction Detection Results

The experiment hypothesized that different factors do not act independently on the spatial distribution of built heritage, and therefore, the seven variables that passed the significance test were subjected to interaction detection. The results of the interaction test indicate that the factors interact and do not act independently. The combination of any two factors enhances the explanatory power of a single dependent variable, resulting in nonlinear or two-factor enhancement (Table 5). Three sets (14.39%) were two-factor enhancements, which were population ∩ number of counties (q = 0.3354) and GDP (q = 0.2294), and river density ∩ number of counties (q = 0.3259). Eighteen sets (85.71%) were nonlinear enhancements. In particular, the combination of topographic relief and population had the greatest effect, i.e., the topographic relief ∩ population had the strongest explanatory power for distribution (q = 0.4265) (Table 5). Comparative observations showed that the geographical distribution of the driving factors was not uniform; multiple influences that reinforced or limited each other arose when confronted with the same built heritage distribution. Thus, the built heritage distribution within the study area was not affected by a single factor but was the result of a multifactorial approach.

Table 5. Results of interaction detection of impact factors.

	Topographic Relief	River Density	Road Density	Population	Population Density	Number of Counties	GDP
Topographic fluctuation	0.1363						
River density	0.3351 ↖	0.1062					
Road density	0.3564 ↖	0.2097 ↖	0.0597				
Population	0.4265 ↖	0.2574 ↖	0.2555 ↖	0.1448			
Population density	0.3187 ↖	0.2275 ↖	0.1877 ↖	0.3281 ↖	0.0938		
Number of counties	0.4106 ↖	0.3259 ↗	0.3435 ↖	0.3354 ↗	0.4097 ↖	0.2354	
GDP	0.3976 ↖	0.2626 ↖	0.2439 ↖	0.2294 ↗	0.3213 ↖	0.4085 ↖	0.1398

Note: ↖ represents a nonlinear enhancement relationship and ↗ represents a two-factor enhancement relationship.

3.3.4. Spatial Variation in the Role of Influencing Factors

To further analyze the spatial differences in the direction and strength of the effects of seven variables that passed the significance test on different city-level spatial units, a geographically weighted regression model was used for local spatial regression analysis to investigate.

(1) Tests for multicollinearity and spatial autocorrelation

Multicollinearity refers to the distortion of the estimation or the difficult estimation of a linear regression model due to the precise or highly correlated relationship between explanatory variables. Multiple covariance tests are performed before MGWR to ensure the validity of the geographically weighted regression model [47]. SPSS 24 was used in this study to test multicollinearity with the number of built heritages as the dependent variable. The results show that the tolerance values of GDP and population are less than 0.2, and the VIF values are greater than five, indicating mild multicollinearity. By using stepwise regression, the population size factor was screened out and ultimately satisfied the test of multicollinearity (Table 6).

Table 6. Multicollinearity test and adjustment results.

Independent Variable	Pre-Adjustment		After Adjustment	
	Tolerance	VIF	Tolerance	VIF
Topographic fluctuation	0.733	1.365	0.789	1.267
River density	0.840	1.190	0.843	1.186
Road density	0.488	2.050	0.488	2.049
Population	0.130	7.688		
Population density	0.364	2.746	0.387	2.582
Number of districts	0.437	2.286	0.753	1.329
GDP	0.189	5.296	0.476	2.102

Note: 0.1 < tolerance < 0.2 and VIF > 5, indicating mild multicollinearity; tolerance < 0.1 and VIF > 10, indicating severe multicollinearity.

The spatial autocorrelation method in ArcGIS 10.8 was used to analyze the clustering and dispersion characteristics of built heritage. The number of built heritages was taken as the research object, and the conceptual model of inverse distance was used to analyze the spatial clustering and dispersion characteristics of built heritage (Table 2). The results show that the *p*-value is 0, indicating a confidence level of 100%; the Moran's I index is 0.356, indicating a positive correlation in the distribution of built heritage in the regions, and has a clear spatial clustering characteristic (Figure 2), making it suitable for further analysis of the influencing factors using the geographically weighted regression model.

(2) Multiscale geo-weighted regression analysis

Considering that the scale of action of the influencing factors is different, MGWR was used to explore the quantitative relationship between the kernel density of built heritage and explanatory variables. The entire modeling and parameter fitting was conducted using MGWR 2.2. Parameterization in MGWR 2.2 utilized an adaptive bisquare kernel with bandwidth optimized via Golden Section Search, aiming to minimize the corrected Akaike Information Criterion (AIC) [39]. Kernel selection was determined by comparing residual spatial autocorrelation, where the bisquare kernel reduced Moran's I by 12.7% significantly and was thus adopted. The optimal bandwidth for the river, road density, and GDP are 348.0000; following is population density (174.000) and number of districts (130.0000), and topographical fluctuation is the smallest (50.000). In addition, the regression coefficients of the explanatory variables in the MWGR experimental results were counted and visualized to analyze their impact on the spatial distribution of the built heritage.

The regression coefficients for topographical fluctuation range from −0.287 to 3.542, with a relative difference (maximum regression coefficient—minimum regression coefficient) of 3.829, which is the largest among the six explanatory variables. There are 90% positive units and 10% negative units. Because of the different sizes of the cities, the units accounted for only 1/2 of the national territory, even though the positive units accounted for 90% of the total. There are obvious differences in the spatial effects. The positive peaks appear in the south-central North China Plain and the Yangtze River Delta region, both located in the third step of Chinese terrain, where topographic relief has a positive and significant effect on the spatial distribution of the built heritage. The negative peaks are distributed in the region to the west of the E110 in China, located in the first and second steps of the Chinese terrain, where topographic relief has a reverse effect on the spatial distribution of the built heritage (Figure 5a). Further, constructive destruction is counterproductive to the preservation of built heritage in the third step of the Chinese terrain, while the constraints on urbanization imposed by the high topographic relief promote the emergence and development of built heritage. The first and second step of the Chinese terrain is characterized by harsh subsistence conditions, where the number of settlements is more clearly influenced by topography. Therefore, the negative impact of high topographic relief on the number of settlements is an important reason for its inverse effect on the number of built heritages.

The regression coefficients for river density range from −0.025 to 0.029, with a relative difference of 0.054, 90% of positive units, and 10% of negative units. In terms of spatial differences, the positive peak was located in Guizhou, Hainan, and western Guangdong, where the rivers had a positive and strongest effect on the spatial distribution of the built heritage. At the same time, the negative peak was located in western Xinjiang and western Tibet, where the rivers had the most pronounced reverse effect on the spatial distribution of the built heritage (Figure 5b).

The regression coefficients for road density range from 0.183 to 0.198, with a relative difference of 0.015. All analysis units have positive regression coefficients, indicating that road network density has a positive effect on the research object nationwide, and the spatial difference is not large. In terms of spatial differences, the peak appeared in the northern region of China, where the positive effect of road density was stronger. The valleys appeared in the regions of Guizhou and Hainan, western Guangdong, and southeastern Guizhou, where the positive effect of the road network density was weaker (Figure 5c).

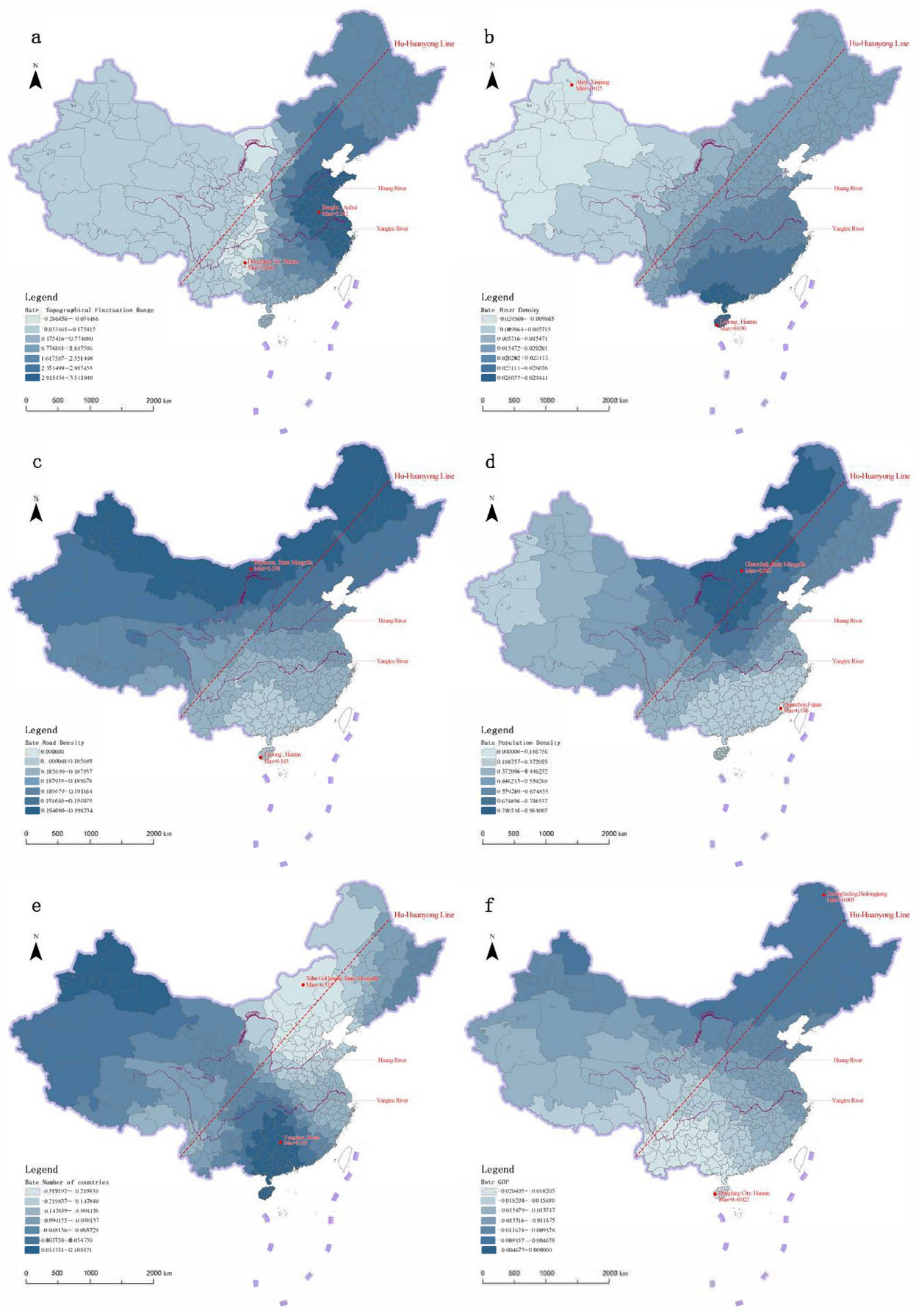


Figure 5. Regression coefficients of the explanatory variables: (**a**) topographical fluctuation range; (**b**) river density; (**c**) road density; (**d**) population density; (**e**) number of counties; (**f**) GDP.

The regression coefficients for population density range from 0.319 to 0.963, with a relative difference of 0.644. Similar to road density, all analysis units have positive regression coefficients, indicating that population density promotes the spatial distribution of built heritage nationwide. In terms of spatial differences, the positive peak was found in Shanxi, northern Shaanxi, western Jixi, and the central-northern part of Inner Mongolia, where the population density played an obvious and positive role. The negative peaks were found in Beijing–Tianjin–Hebei, eastern Shanxi, northern Shanxi, and central Inner Mongolia, where the population density played an inconspicuous and positive role (Figure 5d).

The regression coefficients for the number of counties range from −0.319 to 0.105, with a relative difference of 0.424. There were 27% positive units and 73% negative units. The influence of the number of counties and districts on the built heritage was affected by both cultural protection policies formulated by the provincial government and the level of economic development, with obvious regionality. In terms of spatial differences, the positive peaks are concentrated in two regions. One was Hunan, Guizhou, Hainan, and western Guangdong, and another was northern Xinjiang, where the number of counties played an obvious and positive role. The negative peaks were found in Beijing–Tianjin–Hebei, eastern and northern Shanxi, and central Inner Mongolia, where the number of counties played an inconspicuous and positive role (Figure 5e).

The regression coefficients for GDP range from −0.020 to −0.005, with a relative difference of 0.015. All analysis units have negative regression coefficients, indicating that GDP has an inverse effect on the spatial distribution of the study object at the national level. In terms of spatial differences, the peaks appeared in the Northeast Plain and the Daxing'anling prefecture in Inner Mongolia, where the GDP had the strongest inverse effect. The valleys appeared in the Yunnan–Guizhou Plateau, western Guangxi, and southern Sichuan, where the GDP had the weakest inverse effect (Figure 5f).

4. Discussion

This study employs MGWR and geographical detectors to systematically unravel the complex heterogeneity and multidimensional drivers underlying the spatial distribution of multi-type built heritage in China. Compared to existing studies [4,48], our innovations are threefold.

First, we integrate historical settlements, cultural relics, historic areas, and functional heritage (agricultural/industrial) into a nationwide multi-type database, transcending the limitations of single-type analyses. Second, the MGWR model validates significant spatial heterogeneity in the interaction between natural factors (e.g., topographic relief) and human factors (e.g., number of counties). A regional heterogeneity analysis reveals significant divergence in core drivers (Figure 5): In heritage-intensive zones (e.g., Taihang Mountains, KD_M = 352.8276), topographic barriers synergize with Ming–Qing merchant route policies to enable conservation; conversely, in scarcity zones (e.g., Northwest China), economic stagnation (GDP β = −0.020) and population outflows reduce heritage designation incentives, exemplified by Haixi Prefecture, Qinghai (<0.5 sites/10,000 km^2) [49]. Third, we reveal a potential conflict between economic development (GDP) and heritage preservation, with negative effects (Bate = −0.020~−0.005) most pronounced in the Yangtze River Delta and Pearl River Delta megacities. This aligns with Zhao et al.'s [50] observation of "deindustrialization-driven heritage loss" but further indicates that even economically vibrant regions face development pressures threatening heritage.

The dominance of administrative factors (number of counties, q = 0.2345) highlights—with Yunnan's county-level incentives increasing heritage designation by 23%, while non-policy provinces averaged only 7% growth (2020–2023)—how China's "bottom-up" heritage designation system fundamentally shapes spatial patterns. For example, Yunnan

province—home to the highest number of traditional villages—leverages provincial policies to prioritize heritage registration. However, this mechanism may exacerbate regional imbalances, as underdeveloped western areas struggle with limited administrative resources. GDP's negative effect ($\beta = -0.020$) reveals core development–preservation tensions: (1) direct displacement—rapid urbanization demolishes low-protection heritage (e.g., Yangtze Delta's 2010–2020 industrial relic loss correlates with GDP at $r = 0.91$); (2) mediation—GDP $\rightarrow$ urbanization $\rightarrow$ land value inflation $\rightarrow$ heritage commodification (mediation accounts for 62%); (3) policy buffer—under interventions like Beijing's 'Old City Rehabilitation', GDP may show weak positive effects. Additionally, the nonlinear interaction between topographic relief and population density ($q = 0.4265$) suggests that mountainous regions in central-eastern China (e.g., southern Anhui–western Zhejiang) preserve heritage through "passive conservation" due to constrained urbanization. While this supports a "counter-urbanization" strategy, overreliance on geographic barriers risks disrupting the living inheritance of heritage.

The high explanatory power of county count ($q = 0.2345$) must be contextualized within China's heritage designation policy: first, the 1982–2023 'bottom-up' system made counties screening hubs (e.g., Yunnan's 2016 'One County One Heritage' policy increased traditional villages by 38%), and second, historical path dependence—the Ming Dynasty's 'Lijia System' established county governance that persists in core heritage zones (e.g., Shanxi/Henan heritage density is 2.7$\times$ higher than non-historic counties). These policy–historical confounders partially explain the variable's statistical dominance.

Limitations include the following: First, the lack of historical geographic data (e.g., ancient post roads and ethnic migration routes) may underestimate cultural diffusion's role. For instance, heritage clusters in Qiandongnan Miao–Dong Autonomous Prefecture ($KD_M = 197.5329$) could relate to historical "loose-rein policies" and ethnic autonomy [20], yet such variables are absent in current models. Second, kernel smoothing may obscure sharp terrain transitions (e.g., Sichuan Basin–Hengduan Mountains), though adaptive bandwidths reduced bias. Third, a grid-scale analysis improves natural factor precision but incompletely resolves administrative biases in socio-cultural data (e.g., GDP and population), potentially misrepresenting drivers. Future research should integrate high-resolution historical maps, ethnography, and social media geotags for interdisciplinary frameworks. Furthermore, combining MGWR with deep learning (e.g., convolutional neural networks) could dynamically simulate spatiotemporal heritage evolution and provide early warnings for heritage risk assessment.

5. Conclusions

This study bridges Central Place Theory (heritage clusters as hierarchical nodes) and Cultural Ecology (nature–culture coevolution) through two innovations. (1) Methodological: MGWR's multiscale approach (vs. GWR's rigidity) captures the terrain's local effects ($\beta = 3.542$) and GDP's global trends ($\beta = -0.020$) simultaneously—unachievable in prior single-bandwidth models [39]. (2) Empirical: demonstrates China's 'county-town-village' heritage hierarchy, which mirrors Christaller's $K = 3$ system, but with Confucian governance adaptations. By integrating open internet data and authoritative lists, we constructed a nationwide database of over 40,000 built heritage sites across 31 provinces in China. Using kernel density estimation, the average nearest neighbor index, and the standard deviation ellipse, we analyzed the spatial distribution patterns of built heritage. Based on the Geodetector and MGWR with city-level administrative units as the optimal analytical scale, we revealed the influence and interactions of various driving factors. The following conclusions are drawn:

(1) Built heritage exhibits an "east-dense, west-sparse" macro-pattern rooted in historical settlement patterns and contemporary economic gradients, with four high-density zones (Beijing–Tianjin–Hebei, Shanxi–Henan border, Southeast Guizhou, and Anhui–Zhejiang–Fujian) shaped by topographic tiers and economic gradients. Type-specific variations are evident: historic areas cluster in the Yangtze River Delta (KD_M = 19.8522), while industrial heritage forms sub-clusters in Northeast China's old industrial bases [50].

(2) A city-level analysis offers the highest explanatory power, underscoring the critical role of local administrative capacity (number of counties) in China's heritage designation framework, identifying administrative force (number of counties, q = 0.2345) and road networks (Bate = 0.183~0.198) as core positive drivers, while GDP's global negative effect (Bate = −0.020) warns of development–preservation conflicts. The revealed 'policy-economy-culture' tripartite fractures provide targeted intervention frameworks: preventing overtourism in high-density zones (e.g., Zhangjiajie) and excavating potential heritage in low-density regions (e.g., the Qiangtang section of the Silk Road).

(3) A total of 90% of heritage distributions are governed by factor interactions. Topography–population interplay (q = 0.4265) emphasizes "passive conservation" in central-eastern mountains, whereas water network density–GDP synergy (q = 0.2626) suggests economic zones may disrupt heritage corridors through hydraulic projects.

Crucially, these findings offer transferable insights for global heritage conservation: China's β-GDP = −0.020 validates FAR caps in Hanoi's Old Quarter (Vietnam), county-based empowerment (q = 0.235) templates Brasília's Indigenous Zones (Brazil), and Andean terrain-shielding (coeff. = 3.542) informs no-build zones on slopes >25°—demonstrating how localized anomalies refine universal preservation paradigms.

To achieve systematic conservation and the sustainable development of built heritage, integrated strategies spanning spatial planning, administrative mechanisms, and technological innovation are imperative. Spatially, a "low-intervention + digital" conservation model should be prioritized in third-terrain mountainous regions (e.g., Taihang Mountains where β-GDP = −0.018 vs. national β = −0.020), employing LiDAR for 3D heritage documentation and establishing "heritage resilience buffers" to mitigate large-scale developmental disruptions. Administratively, incentives for county-level heritage designation under the Regulations on the Protection of Famous Historical and Cultural Cities, Towns, and Villages should be enhanced, complemented by a dedicated fund for western China to address regional inequities through fiscal transfers. Technologically, integrating the MGWR model into China's "One Map" territorial planning platform would enable the real-time monitoring of development pressures in heritage-rich zones, while blockchain technology ensures tamper-proof data authentication, laying the groundwork for smart heritage governance.

Author Contributions: Y.L.: study design, data curation, spatial analysis, writing, and funding coordination. L.T.: study design, spatial analysis, and funding coordination. Q.H.: visualization and literature review. J.D.: methodological guidance and validation. Z.S.: project administration and funding coordination. L.L.: literature review and funding coordination. All authors have read and agreed to the published version of the manuscript.

Funding: This research was supported by the Department of Education of Henan Province, China, grant no. 2025-ZDJH-427.

Institutional Review Board Statement: Not applicable: this study utilized publicly available geographic and statistical data; no ethical approval was required.

Informed Consent Statement: This study did not involve human participants, personal privacy data, or biological sample collection. All analyzed data were obtained from publicly accessible geospatial and statistical sources. As such, informed consent was not required.

Data Availability Statement: Raw data sources: lists from the National Cultural Heritage Administration and the Ministry of Housing, and gridded GDP/population data from the Chinese Academy of Sciences. Processed spatial data and analysis scripts are available upon request from the corresponding author.

Conflicts of Interest: The authors declare no conflicts of interest.

References

1. Ashworth, J.G. *From History to Heritage—From Heritage to Identity: In Search of Concepts and Models*; Routledge: London, UK, 1994.
2. Abebe, A.H.; Gatisso, M.M. The conservation and preservation challenges and threats in the development of cultural heritage: The case of the Kawo Amado Kella Defensive Wall (KAKDW) in Wolaita, Southern Ethiopia. *Heliyon* **2023**, *9*, e18839. [CrossRef] [PubMed]
3. Graham, B.; Ashworth, G.; Tunbridge, J. *A Geography of Heritage: Power, Culture and Economy*; Routledge: London, UK, 2000.
4. Zeng, C.; Liu, P.; Li, B.; Huang, X.; Cao, Y. Temporal and Spatial Distribution Characteristics and Influencing Factors of Industrial Heritage in China: A Case Study of the Four Batches of Industrial Heritage Lists. *Trop. Geogr.* **2022**, *42*, 740–750.
5. Agnoletti, M.; Santoro, A. The Italian National Register of Historical Rural Landscapes. In *Cultural Heritage—Possibilities for Land-Centered Societal Development*; Springer International Publishing: Cham, Switzerland, 2022; pp. 15–34.
6. Versaci, A. The Evolution of Urban Heritage Concept in France, between Conservation and Rehabilitation Programs. *Procedia Soc. Behav. Sci.* **2016**, *225*, 3–14. [CrossRef]
7. Rourke, G.D. International Council on Monuments and Sites (ICOMOS) (Museums). In *Encyclopedia of Global Archaeology*; Springer International Publishing: Cham, Switzerland, 2014.
8. Ghanbari, E.; Lotfi, S.; Sholeh, M. HUL values in practice: A character area designation model for the conservation of built heritage in less-developed regions. *J. Cult. Herit.* **2024**, *70*, 41–53. [CrossRef]
9. Njoh, A.J. Urbanization and development in sub-Saharan Africa. *Cities* **2003**, *20*, 167–174. [CrossRef]
10. Geng, N.; Wang, X.; Shao, X. Analysis on Spatial Distribution and Influencing Factors of Traditional Villages in Taihang Mountain Area—Taking an Example of Taihang Plate in Shanxi Province. *J. Shanxi Norm. Univ. (Nat. Sci. Ed.)* **2022**, *36*, 70–79.
11. Li, M.; Wu, B.; Cai, L. Tourism development of World Heritage Sites in China: A geographic perspective. *Tour. Manag.* **2008**, *29*, 308–319. [CrossRef]
12. Hutson, J.; Weber, J.; Russo, A. Digital Twins and Cultural Heritage Preservation: A Case Study of Best Practices and Reproducibility in Chiesa dei SS Apostoli e Biagio. *Art Des. Rev.* **2023**, *11*, 15–41. [CrossRef]
13. Winter, T. The geocultural heritage of the Silk Roads. *Int. J. Herit. Stud.* **2020**, *27*, 700–719. [CrossRef]
14. Ghaith, K. AI Integration in Cultural Heritage Conservation–Ethical Considerations and the Human Imperative. *Int. J. Emerg. Disruptive Innov. Educ. VISIONARIUM* **2024**, *2*, 6. [CrossRef]
15. Tam, L.; Whitman, C.J.; Prizeman, O. Global Climate Change and Built Heritage. *Built Herit.* **2025**, *9*, 17. [CrossRef]
16. Wang, R.; Yan, H.; Zhou, L.; Duan, H.; Sun, L. Spatial Distribution Pattern and Driving Factors of Chinese Historical Cultural Towns and Villages. *J. Lanzhou Jiaotong Univ.* **2019**, *38*, 108–114.
17. Wu, Y.; Wu, M.; Wang, Z.; Zhang, B.; Li, C.; Zhang, B. Distribution of Chinese traditional villages and influencing factors for regionalization. *Cienc. Rural* **2021**, *51*, e20200124. [CrossRef]
18. Jia, A.; Liang, X.; Wen, X.; Yun, X.; Ren, L.; Yun, Y. GIS-Based Analysis of the Spatial Distribution and Influencing Factors of Traditional Villages in Hebei Province, China. *Sustainability* **2023**, *15*, 9089. [CrossRef]
19. Li, M.; Ouyang, W.; Zhang, D. Spatial Distribution Characteristics and Influencing Factors of Traditional Villages in Guangxi Zhuang Autonomous Region. *Sustainability* **2022**, *15*, 632. [CrossRef]
20. Liu, W.; Xue, Y.; Shang, C. Spatial distribution analysis and driving factors of traditional villages in Henan province: A comprehensive approach via geospatial techniques and statistical models. *Herit. Sci.* **2023**, *11*, 185. [CrossRef]
21. Jin, L.; Wang, Z.; Chen, X. Spatial Distribution Characteristics and Influencing Factors of Traditional Villages on the Tibetan Plateau in China. *Int. J. Environ. Res. Public Health* **2022**, *19*, 13170. [CrossRef]
22. Li, B.; Wang, J.; Jin, Y. Spatial Distribution Characteristics of Traditional Villages and Influence Factors Thereof in Hilly and Gully Areas of Northern Shaanxi. *Sustainability* **2022**, *14*, 15327. [CrossRef]

23. Li, S.; Song, Y.; Xu, H.; Li, Y.; Zhou, S. Spatial Distribution Characteristics and Driving Factors for Traditional Villages in Areas of China Based on GWR Modeling and Geodetector: A Case Study of the Awa Mountain Area. *Sustainability* **2023**, *15*, 3443. [CrossRef]
24. Montes, L.; Sebastián, M.; Domingo, R.; Beguería, S.; García-Ruiz, J.M. Spatial distribution of megalithic monuments in the subalpine belt of the Pyrenees: Interpretation and implications for understanding early landscape transformation. *J. Archaeol. Sci. Rep.* **2020**, *33*, 102489. [CrossRef]
25. Xi, X.S.; Xu, L.Y.; Chen, Y.Y. Spatial Distribution Characteristics of National Cultural Relic Protection Units. *Hum. Geogr.* **2013**, *28*, 75–79.
26. Gao, H.; Wang, Y.; Zhang, H.; Huang, J.; Yue, X.; Chen, F. Spatial Distribution and Typological Classification of Heritage Buildings in Southern China. *Buildings* **2023**, *13*, 2025. [CrossRef]
27. Li, T.; Li, C.; Zhang, R.; Cong, Z.; Mao, Y. Spatial Heterogeneity and Influence Factors of Traditional Villages in the Wuling Mountain Area, Hunan Province, China Based on Multiscale Geographically Weighted Regression. *Buildings* **2023**, *13*, 294. [CrossRef]
28. Huang, X.; Feng, Y.; Li, D.; Li, Z.; Wang, W. Analysis on the spatial distribution characteristics of traditional villages in northwest China. *J. Northwest Norm. Univ. (Nat. Sci.)* **2018**, *54*, 117–123.
29. Ciolac, R.; Adamov, T.; Iancu, T.; Popescu, G.; Lile, R.; Rujescu, C.; Marin, D. Agritourism—A Sustainable Development Factor for Improving the 'Health' of Rural Settlements. Case Study Apuseni Mountains Area. *Sustainability* **2019**, *11*, 1467. [CrossRef]
30. Karawapong, A.; Karoonsoontawong, A.; Kanitpong, K. Exploring the multiscale relationship between the built environment and metro station ridership. *Case Stud. Transp. Policy* **2025**, *20*, 101466. [CrossRef]
31. Lin, J.; Liu, S.; Zheng, S.; Lai, N.; Wu, X. Accessibility and Influencing Factorsof Traditional Villages in Fujian Province Based on GWR Model. *J. Chin. Urban For.* **2023**, *21*, 144–148.
32. Fu, Q.; Yang, Z.; Dong, S.C.; Yang, H.X.; Niu, Z.H.; Xu, W.L. Research on spatial accessibility and influencing factors of national traditional villages in Henan Province. *J. Henan Norm. Univ. (Nat. Sci. Ed.)* **2021**, *49*, 82–90.
33. Pietrostefani, E.; Holman, N. The politics of conservation planning: A comparative study of urban heritage making in the Global North and the Global South. *Prog. Plan.* **2021**, *152*, 100505. [CrossRef]
34. Wang, J.; Xu, C. Geodetector: Principle and prospective. *Acta Geogr. Sin.* **2017**, *72*, 116–134.
35. Elkady, A.H.; Abdrabou, A.S.; Elayouty, A. Multiscale geographically weighted quantile regression. *Spat. Econ. Anal.* **2025**, 1–24. [CrossRef]
36. Mansour, S.; Al Kindi, A.; Al-Said, A.; Al-Said, A.; Atkinson, P. Sociodemographic determinants of COVID-19 incidence rates in Oman: Geospatial modelling using multiscale geographically weighted regression (MGWR). *Sustain. Cities Soc.* **2021**, *65*, 102627. [CrossRef] [PubMed]
37. Tomal, M. Exploring the meso-determinants of apartment prices in Polish counties using spatial autoregressive multiscale geographically weighted regression. *Appl. Econ. Lett.* **2022**, *29*, 822–830. [CrossRef]
38. Kurkcuoglu, M.A. Analysis of the energy justice in natural gas distribution with Multiscale Geographically Weighted Regression (MGWR). *Energy Rep.* **2023**, *9*, 325–337. [CrossRef]
39. Fotheringham, A.S.; Yang, W.; Kang, W. Multiscale Geographically Weighted Regression (MGWR). *Ann. Am. Asso-Ciation Geogr.* **2017**, *107*, 1247–1265. [CrossRef]
40. Turner, B.L.; Kasperson, R.E.; Matson, P.A.; McCarthy, J.J.; Corell, R.W.; Christensen, L.; Eckley, N.; Kasperson, J.X.; Luers, A.; Martello, M.L.; et al. Science and Technology for Sustainable Development Special Feature: A framework for vul-nerability analysis in sustainability science. *Proc. Natl. Acad. Sci. USA* **2003**, *100*, 8074–8079. [CrossRef]
41. Lefebvre, H. *The Production of Space*; Wiley-Blackwell: Hoboken, NJ, USA, 1991.
42. Salazar, L.G.; Figueiredo, R.; Romão, X. Flood vulnerability assessment of built cultural heritage: Literature review and identification of indicators. *Int. J. Disaster Risk Reduct.* **2024**, *111*, 104666. [CrossRef]
43. Guzman, P. Cultural heritage in climate planning: An analysis of the Norwegian national climate documents and guidelines. *J. Cult. Herit.* **2025**, *74*, 35–47. [CrossRef]
44. Zhao, Y. Spatial Distribution Characteristics and Influencing Factors of Industrial Heritage in China. *Archit. Cult.* **2020**, *9*, 88–91.
45. Yang, M.; Feng, X. Study on Temporal and Spatial Distribution and Influencing Factors of Key Rural Tourism Villages in China. *J. Yibin Univ.* **2023**, *23*, 43–53.
46. Tian, J.J.; Zhang, J.S. Research on Spatial-Temporal Distribution and the Driving Factors of CO_2 Emissions in China Based on Geographic Detector. *Ecol. Econ.* **2022**, *38*, 13–20+27.
47. Mandal, B.; Goswami, K.P. Evaluating the influence of biophysical factors in explaining spatial heterogeneity of LST: Insights from Brahmani-Dwarka interfluve leveraging Geodetector, GWR, and MGWR models. *Phys. Chem. Earth Parts A/B/C* **2024**, *138*, 103836. [CrossRef]

48. Chen, B.; Xu, S.Z.; Zhou, Y.Y.; Wang, H.Z.; Yang, D.T.; Ye, Y.Q. Analysis of Multi-scale Characteristics and Influencing Factors Under the Spatial Distribution of Traditional Villages—Taking 263 Traditional Villages in Guangdong Province as Examples. *Res. Soil Water Conserv.* **2023**, *30*, 423–429.
49. Xu, H.; Wang, J.; Jin, S. Spatial Distribution and Tourism Response of Cultural Heritage in Shandong Province: Taking the Cultural Heritage Protection Unit as an Example. *J. Ludong Univ. (Nat. Sci. Ed.)* **2022**, *38*, 320–328+356.
50. Zhao, Q.; Li, H. Research on spatial differentiation characteristics and formation mechanism of national industrial herit-ages. *Urban Probl.* **2022**, *11*, 54–64.

Disclaimer/Publisher's Note: The statements, opinions and data contained in all publications are solely those of the individual author(s) and contributor(s) and not of MDPI and/or the editor(s). MDPI and/or the editor(s) disclaim responsibility for any injury to people or property resulting from any ideas, methods, instructions or products referred to in the content.